Macromolecular Research, Vol. 11, No. 1, pp 53-61 (2003)

Salt-Induced Protein Precipitation in Aqueous Solution: Single and Binary Protein Systems

Sang Gon Kim and Young Chan Bae*

Division of Chemical Engineering and Molecular Thermodynamics Lab., Hanyang University, Seoul 133-791, Korea

Received Dec. 7, 2002; Revised Jan. 24, 2003

Abstract: A molecular-thermodynamic model is developed for the salt-induced protein precipitation. The protein molecules interact through four intermolecular potentials. An equation of state is derived based on the statistical mechanical perturbation theory with the modified *Chiew's* equation for the fluid phase, Young's equation for the solid phase as the reference system and a perturbation based on the protein-protein effective two body potential. The equation of state provides an expression for the chemical potential of the protein. In a single protein system, the phase separation is represented by fluid-fluid equilibria. The precipitation behaviors are simulated with the partition coefficient at various salt concentrations and degree of pre-aggregation effect for the protein particles. In a binary protein system, we regard the system as a fluid-solid phase equilibrium. At equilibrium, we compute the reduced osmotic pressure-composition diagram in the diverse protein size difference and salt concentrations.

Keywords: protein, interaction potentials, precipitation, phase equilibria, pre-aggregation, perturbation, salt.

Introduction

In early days of protein chemistry, the only practical way of separating different types of protein was by precipitating part of a mixture through the alternation of some property of the solvent. Protein precipitation is the simplest and the oldest practical way to separate different proteins from a solution mixture. Separation is achieved through the addition of precipitation agents such as inorganic salts, nonionic polymers, polyelectrolytes, and organic solvents.[1-5]

A variety of researches on the protein precipitation behavior have been studied by using various experimental techniques. Shih *et al.*[3] observed the solubility of lysozyme, α-chymotrypsin and bovine serum albumin in an aqueous electrolyte solution as a function of ionic strength, pH, the chemical nature of salt, and the initial protein concentration. Coen *et al.*[6] studied the salting-out phase equilibria for lysozyme and α-chymotrypsin from the concentrated ammonium-sulfate solution. Their experimental results suggest that the protein salting-out may be considered a fluid-fluid phase separation resulting in a supernatant fluid phase with a dense precipitate fluid phase. The degree of separation is characterized by the partition coefficient, K, which is defined as the ratio of the protein concentration in the dense phase to that in the supernatant phase.

Theoretically, many researchers(Verwey and Overbeek, 1948; Asakura and Oosawa, 1958; Vrij, 1976; Joanny *et al.*, 1979; De Hek and Vrij, 1995; Gast *et al.*, 1983b; Grimson, 1983; Victor and Hansen, 1984)[7-14] reported models to describe the phase behaviors of these complex systems by using the one-component mean-force potential approximation. Mahadevan and Hall,[15,16] Vlachy and Prausnitz[17,18] have used the model to describe the phase behavior of aqueous globular proteins in solutions at low salt concentration, and Chiew *et al.*[19] and Kuehner *et al.*[20] used a similar approach for solutions at high salt concentartion. Thermodynamic model with a properly chosen potential of mean force leads to a satisfactory description of the phase behavior of a protein solution. Thermodynamic properties and phase-separation conditions of protein solutions described by such model have been computed using a number of different satistical-mechanical approximation methods. These methods can be charaterized as based on the osmotic virial expansion, statistical-mechanical perturbation theory, integral-equation theory, and the random-phase approximation.

By using the second-order Baker and Henderson perturbation theory with the Asakura Oosawa osmotic attraction[8,21] as the dominant contribution of the mean force potential, Gast *et al.*[22] and Mahadevan and Hall[16] have studied the polymer-induced phase separations of aqueous colloidal, nonaqueous colloidal and nonadsorbed protein systems. Predictions based on this method led to solid-fluid phase

*e-mail : ycbae@hanyang.ac.kr

transition rather than fluid-fluid phase separation observed experimentally by de Hek and Vrij[11] for colloidal systems. However, They have shown that the perturbation theory combined with the Asakura-Oosawa potential is able to predict both fluid-fluid and solid-fluid transitions when very large polymer molecules are present.

Based on the experimental studies of de Hek and Vrij[11] for colloidal systems and of Shih *et al.*[3] for protein solutions, it suggests that a salt- (or polymer-) induced protein (or colloid) precipitation may be more appropriately viewed as a phase separation resulting in two fluid phases. Grimson,[13] Vlachy *et al.*,[18] Chiew *et al.*[19] and Kuehner *et al.*[20] have used the random-phase approximation to describe a fluid-fluid phase separation for a similar mean-force potential to that used in the previously mentioned perturbation theory calculatioins. The major advantage of the random-phase approximation is its simplicity; little computational effort is required to calculate the whole phase diagram.

In this study, we present a molecular-thermodynamic framework for the protein precipitation by inorganic salt. The summary of our works is as follow:

(1) We describe the single protein system with a fluid-fluid phase equilibrium. The equilibrium model represents the solution as a pseudo-one component system containing only a continuous solvent and a globular protein. Our equation of state is the sum of a hard-sphere reference contribution and a perturbation. The reference term is derived by the modified *Chiew*'s model to describe the pre-aggregating effect[30, 31] of protein. Protein-protein effective two-body potentials are also discussed. These potentials include Coulombic repulsion, dispersion attraction, osmotic attraction, and attractive specific potential to represent specific chemical interactions. The determination of reasonable values of degree of pre-aggregation effect is accomplished by correlating our model with the partition coefficient-ionic strength data.[6]

(2) We develop a molecular-thermodynamic model to compute phase behaviors of the binary protein systems that contain two types of globular proteins in addition to the solvent. An eq. of state is derived based on the perturbation theory. The reference term is derived using the simplified *Chiew*'s equation in the fluid phase and the Young's equation in the solid phase. The perturbation equation is given as the same as for the single protein system for both fluid and solid phases. The energy difference between two phases is represented by the disparity of the protein density. The influence of the protein size difference and salt concentration is also discussed.

Theoretical Consideration

Protein-Protein Potentials. The overall effective two-body potential between two different protein molecules, $W_{ij}^{overall}$, is given by the sum of four potentials.

$$W_{ij}^{overall}(r) = W_{ij}^{elec}(r) + W_{ij}^{disp}(r) + W_{ij}^{osmotic}(r) + W_{ij}^{specific}(r) \quad (1)$$

where r is the center to center separation length. $W_{ij}^{elec}(r)$ is the electric double-layer-repulsion potential, $W_{ij}^{disp}(r)$ is the dispersion potential of Hamaker, $W_{ij}^{osmotic}(r)$ is an attractive interaction due to the excluded-volume effect of the salt ions, and $W_{ij}^{specific}(r)$ is an attractive potential between proteins representing any specific chemical effects such as hydrophobic interactions. Appendix provides expressions for the various potentials of mean force.

Figure 1 shows a representative overall protein-protein perturbation potential of mean force, when the ionic strength is 0.01 M (a), and the effect of electric repulsive potential disappears when the ionic strength is 5 M (b).

This means that the electric double-layer potential has the repulsive interaction between particles. At high ionic strength, however, it can be negligible. As the ionic strength increase, the osmotic interaction potential greatly increases to the negative direction. At extremely low ionic strength, therefore, total interaction potential can be repulsive and salting-in region can be observed.

Equation of State. In perturbation theory, an assembly of hard spheres is used as the reference system, while the

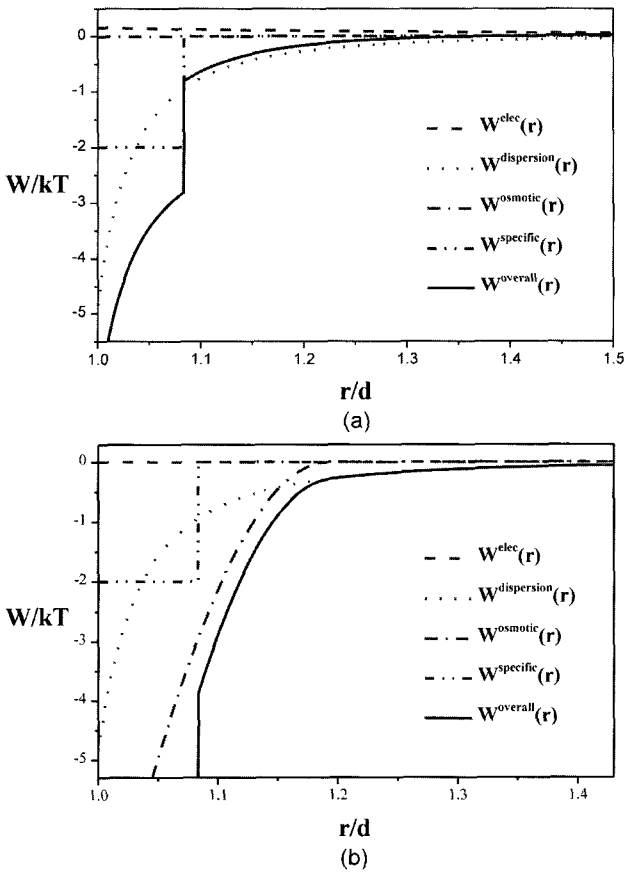

Figure 1. Contribution to the total effective two-body potential as a function of r/d in the case of $I = 0.01$ M (a) and $I = 5$ M (b): pH = 7, $H/kT = 8.9$, $\varepsilon_{sp}/kT = 2$, $\delta = 0.3$ nm, $d_s = 0.694$ nm, $d = 3.44$ nm, $C_{salt} = 5$ M.

remaining interactions are treated as perturbations;

$$\frac{P}{\rho kT}=\left(\frac{P}{\rho kT}\right)_{ref}+\left(\frac{P}{\rho kT}\right)_{pert} \tag{2}$$

where ρ is the density of protein molecules, and P is the pressure.

Single Protein System. In aqueous solution, protein particles folded to sphere and dispersed as the colloidal dispersion. In this case, protein molecules are not absolutely dispersed to only single type of protein particles, but have some portion of dimer or trimer. This effect is called pre-aggregation.

The reference system is given by the modified *Chiew*'s equation[19] to consider pre-aggregation effect:

$$\left(\frac{P}{\rho kT}\right)_{ref}=1+4\omega_{PA}\eta\frac{1-\frac{\eta}{2}}{(1-\eta)^3}-(\omega_{PA}-1)\left[\frac{1-\frac{\eta}{2}}{(1-\eta)^3}-1\right] \tag{3}$$

where η is the packing fraction, given by $\eta=\pi\rho d^3/6$, where d is the diameter of single protein, ω_{PA} represents the average degree of pre-aggregation that is reduced by the hydrophobic part of the protein surface.

The perturbation term is

$$\left(\frac{P}{\rho kT}\right)_{pert}=\frac{\omega_{PA}^2\rho U}{2kT} \tag{4}$$

where U is the perturbation energy per unit density, given (for a single-protein system) by

$$U=4\pi\int W_{i=j}^{overall}(r)r^2dr \tag{5}$$

where $W_{i=j}^{overall}(r)$ is the overall protein-protein effective two-body potential defined in eq. (1). The total equation is, therefore,

$$\left(\frac{P}{\rho kT}\right)_{ref}=1+4\omega_{PA}\eta\frac{1-\frac{\eta}{2}}{(1-\eta)^3}-(\omega_{PA}-1)\left[\frac{1-\frac{\eta}{2}}{(1-\eta)^3}-1\right]+\frac{\omega_{PA}^2\rho U}{2kT} \tag{6}$$

The general eq. for calculating the Helmholtz energy from a pressure-explicit equation of state[23] is

$$A(T,V)=A^{\circ}(T)+\int_V^{\infty}\left(P-\frac{NkT}{V}\right)dV+kTNln\left(\frac{NkT}{V}\right) \tag{7}$$

Eq. (7) can be written in terms of T and ρ.

$$\frac{A}{N\omega_{PA}kT}=\frac{A^{\circ}}{N\omega_{PA}kT}+\int_0^{\rho\omega_{PA}}\left(\frac{P}{\rho\omega_{PA}kT}-\frac{1}{\omega_{PA}}\right)\frac{d(\rho\omega_{PA})}{\rho\omega_{PA}}+ln(\rho\omega_{PA}kT) \tag{8}$$

Then, the chemical potential is

$$\mu=\left(\frac{\partial A}{\partial N}\right)_{T,V} \tag{9}$$

$$\begin{aligned}\frac{\Delta\mu}{kT}&=\frac{\mu}{kT}-\frac{\mu^o}{kT}=\left(\frac{\Delta\mu}{kT}\right)_{ref}+\left(\frac{\Delta\mu}{kT}\right)_{pert}\\&=8\omega_{PA}\eta\frac{4-3\eta}{4(1-\eta)^2}+4\omega_{PA}\eta^2\frac{5-3\eta}{4(1-\eta)^3}+(\omega_{PA}-1)ln(1-\eta)\\&-(\omega_{PA}-1)\frac{5-4\eta}{4(1-\eta)^2}-(\omega_{PA}-1)\frac{2\eta^3-6\eta^2+5\eta}{2(1-\eta)^3}\\&+ln\rho+1+\frac{\omega_{PA}^2\rho U}{kT}\end{aligned} \tag{10}$$

At equilibrium, protein concentrations in the supernatant and dense-fluid phases are calculated from eqs. (6) and (10) based on the classical equilibrium conditions:

$$\Delta\mu^s=\Delta\mu^d \tag{11}$$

$$P^s=P^d \tag{12}$$

where superscripts "s" and "d" denote the supernatant and dense phases, respectively.

Binary Protein System. Derivation of the equation of state for mixtures follows a rigorous first-order statistical-mechanical perturbation theory based on the mixture of hard-spheres as a reference system. In binary protein system, fluid-solid phase separation is dealt with protein-poor phase and protein-rich phase separation.[24]

Fluid Phase: The equation of state for fluid mixtures is written as

$$\left(\frac{P}{kT}\right)_{fluid}=\left(\frac{P}{kT}\right)_{fluid,ref}+\left(\frac{P}{kT}\right)_{fluid,pert} \tag{13}$$

The reference system is given by the extension of eq. (6) with the simple case, $\omega_{PA}=1$.

$$\left(\frac{P}{\rho kT}\right)_{ref}=1+\rho\sum_{ij}^{m}x_ix_jb_{ij}g_{ij}(d_{ij}^{+}) \tag{14}$$

where $x_i=N_i/N$ is the number fraction of molecules, $g_{ij}(d_{ij}^{+})$ is the ij pair radial distribution function of hard-sphere mixtures at contact and b_{ij} is the combining second virial coefficient of hard sphere

$$b_{ij}=\frac{2\pi}{3}d_{ij}^3 \tag{15}$$

where d_{ij} is the combining effective hard sphere diameter

$$d_{ij} = \frac{d_{ii} + d_{jj}}{2} \tag{16}$$

where d_{ii} and d_{jj} are the effective hard-sphere diameters for pure fluids i and j.

To obtain explicit equation of state from eq. (14), a suitable mathematical form[25] for $g_{ij}(d_{ij}^{+})$ is needed.

$$g_{ij}(\eta, \xi_{ij}) = \frac{1}{1-\eta} + \frac{3}{2}\frac{\xi_{ij}}{(1-\eta)^2} + \frac{1}{2}\frac{\xi_{ij}^2}{(1-\eta)^3} \tag{17}$$

In protein mixtures, the packing fraction η is defined by:

$$\eta = \frac{\rho}{4}\sum_{i}^{m} x_i b_{ii} \tag{18}$$

$$\xi_{ij} = \left(\frac{b_{ii}b_{jj}}{b_{ij}}\right)^{1/3} \frac{\rho}{4}\sum_{k}^{m} x_k b_{kk}^{2/3} \tag{19}$$

For one-component systems and equal-segment-size mixtures, $\xi_{ij} = \eta$, and eq. (14) reduces to the Carnahan-Starling eq. for hard spheres.[26]

The perturbation term is

$$\left(\frac{P}{\rho kT}\right)_{pert} = \frac{\rho U^{total}}{2kT} \tag{20}$$

where U^{total}/kT is the total interaction energy of all pairs

$$\frac{U^{total}}{kT} = \sum_{i,j=1}^{m} x_i x_j \frac{U_{ij}^{total}}{kT} \tag{21}$$

where x_i is the mole fraction of the component i and U_{ij}^{total} is the total interaction energy for i-j pair.

$$\frac{U_{ij}^{total}}{kT} = 4\pi\int_{d_{ij}+2\Delta r}^{\infty}\left[\frac{W_{ij}^{overall}(r)}{kT} r^2\right]dr \tag{22}$$

where $W_{ij}^{overall}(r)$ is the protein-protein effective two-body potential for the i-j pair. Therefore, the total equation of state, the sum of the reference term and the perturbation term, is given by

$$\left(\frac{P}{\rho kT}\right) = 1 + \rho\sum_{ij}^{m} x_i x_j b_{ij} g_{ij}(d_{ij}^{+}) + 2\pi\rho\sum_{ij}^{m}\left(x_i x_j \int \frac{W_{ij}^{overall}}{kT} r^2 dr\right) \tag{23}$$

The general equation for calculating the Helmholtz energy from equation of state is

$$\frac{A}{NkT} = \sum_{i}^{m} x_i \frac{A_i^o}{N_i kT} + \int_0^{\rho}\left(\frac{P}{\rho kT} - 1\right)\frac{d\rho}{\rho} + \sum_{i}^{m} x_i ln(x_i \rho kT) \tag{24}$$

The final form is

$$\frac{A}{NkT} = \sum_{i}^{m} x_i \frac{A_i^o}{NkT} + \rho x_i x_j b_{ij} W_{ij} + \frac{\rho U^{total}}{2kT} \tag{25}$$

Then, the chemical potential is

$$\Delta\mu_k = \left(\frac{\partial A}{\partial N_k}\right)_{T,V,N_{i\neq k}} \tag{26}$$

The result is

$$\left(\frac{\Delta\mu_k}{k_B T}\right)_{ref} = 2\rho\sum_{i=1}^{m} x_i b_{ik} Q_{ik} + \rho\sum_{i,j=1}^{m} x_i x_j b_{ij} \times\left(N\frac{\partial Q_{ij}}{\partial N_k}\right) + ln(x_k \rho kT) + 1 \tag{27}$$

where,

$$Q_{ij} = \frac{I_1}{\eta} + \frac{3}{2}\frac{\xi_{ij}}{\eta^2} I_2 + \frac{1}{2}\frac{\xi_{ij}^2}{\eta^3} I_3 \tag{28}$$

$$\left(N\frac{\partial Q_{ij}}{\partial N_k}\right) = \left(\frac{\partial Q_{ij}}{\partial \eta}\right)\left(N\frac{\partial \eta}{\partial N_k}\right) + \left(\frac{\partial Q_{ij}}{\partial \xi_{ij}}\right)\left(N\frac{\partial \xi_{ij}}{\partial N_k}\right) \tag{29}$$

$$I_1 = -ln(1-\eta),\ I_n = -I_{n-1} + \frac{1}{1-\eta}\frac{\eta^{n-1}}{(1-\eta)^{n-1}} \tag{30}$$

Solid Phase For the solid phase, the reference equation of state and Helmholtz energy are given by[24]:

$$\left(\frac{P}{kT}\right)_{ref} = \rho\left[\frac{3}{V^*-1} + 2.566 + 0.55(V^*-1) - 1.19(V^*-1)^2 + 5.59(V^*-1)^3\right] - 5.95V^{*3}/3 + 15.022 + \sum_{i=1}^{2} x_i ln(x_i) \tag{31}$$

$$\left(\frac{A}{NkT}\right)_{ref} = -3ln\left(\frac{V^*-1}{V^*}\right) + 5.124 ln(V^*) - 20.78V^* + 9.52V^{*2} - 5.95V^{*3}/3 + 15.022 + \sum_{i=1}^{2} x_i ln x_i \tag{32}$$

where $V^* = V/V_0$, $V_0 = Nd_0^3/\sqrt{2}$: $d_0^3 = x_1^2 d_{11}^3 + 2f(\alpha)x_1 x_2 d_{12}^3 + x_2^2 d_{22}^3$.

Here, parameter α is the ratio of smaller to larger hard-sphere diameters. In this work, $d_{11} \geq d_{22}$ is used so that $\alpha = d_{22}/d_{11}$ and the function $f(\alpha)$ is determined approximately to fit the computer-generated fluid-solid coexistence curves for binary hard-sphere mixtures in the range $0.85 \leq \alpha \leq 1$.[24]

$$f(\alpha) = 1 + 13.5(1-\alpha)^{2.5} \tag{33}$$

Eqs. (31) and (32) are based on the fit to the computer generated compressibility factor for an one-component hard-sphere melting point. The chemical potential of component k is defined by

$$\left(\frac{\Delta\mu_k}{kT}\right)_{ref}=\left(\frac{A}{NkT}\right)_{ref}+\left[3\frac{1}{V^*(1-V^*)}+5.124\frac{1}{V^*}-5.95V^{*2}+19.04V^*-20.78\right]\times\left(N\frac{\partial V^*}{\partial N_k}\right)+15.022+ln(x_k) \quad (34)$$

The perturbation of the solid phase is the same as that of the fluid phase, but the energy is represented by the difference of the number density.

The total equations, therefore, are

$$\left(\frac{P}{kT}\right)=\left(\frac{P}{kT}\right)_{ref}+\left(\frac{P}{kT}\right)_{pert}$$
$$=\rho\left[\frac{3}{V^*-1}+2.566+0.55(V^*-1)-1.19(V^*-1)^2+5.59(V^*-1)^3\right]-5.95V^{*3}/3+15.022+\sum_i^m x_i ln(x_i)$$
$$+2\pi\rho^2\sum_{ij}^m\left(x_ix_j\int\frac{W_{ij}^{overall}}{kT}r^2dr\right) \quad (35)$$

$$\left(\frac{\Delta\mu_k}{kT}\right)=\left(\frac{\Delta\mu_k}{kT}\right)_{ref}+\left(\frac{\Delta\mu_k}{kT}\right)_{pert}$$
$$=\left(\frac{A}{NkT}\right)_{ref}+\left[3\frac{1}{V^*(1-V^*)}+5.124\frac{1}{V^*}-5.95V^{*2}+19.04V^*-20.78\right]\times\left(N\frac{\partial V^*}{\partial N_k}\right)+15.022+ln(x_k)$$
$$+4\pi\rho\sum_i^m\left(x_i\int\frac{W_{ki}^{overall}}{kT}r^2dr\right) \quad (36)$$

For aqueous solutions containing two kinds of proteins, the equilibrium condition is

$$\Delta\mu_1^{fluid}=\Delta\mu_1^{solid} \quad (37)$$

$$\Delta\mu_2^{fluid}=\Delta\mu_2^{solid} \quad (38)$$

$$P^{fluid}=P^{solid} \quad (39)$$

where subscripts "1" and "2" represent species of proteins.

Results and Discussion

Single Proetin System. For the precipitation of a single protein in an aqueous salt solution, we examine the effect of ionic strength in phase-separation systems. The partition coefficient, K, of the protein system can be obtained from the equilibrium conditions and is given by the ratio of the equilibrium number density of protein in the dense phase to that in the supernatant phase [$K=\rho_d/\rho_s=\eta_d/\eta_s$].

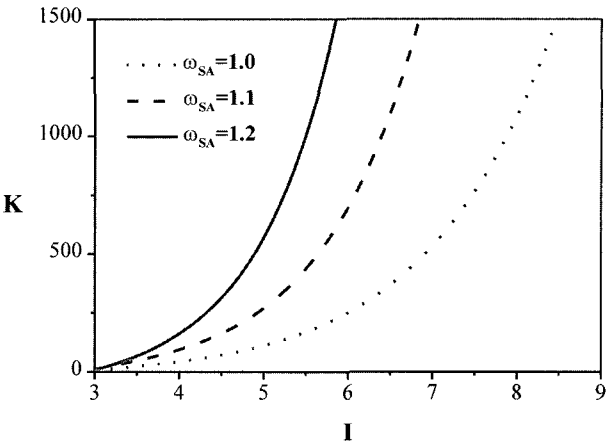

Figure 2. Effect of ionic strength: pH = 7, H/kT = 8.9, ε_{sp}/kT = 2, δ = 0.3 nm, d_s = 0.694 nm, d = 3.44 nm, C_{salt} = 5 M.

Figure 2 shows the predicted partition coefficient K plotted as a function of ionic strength for systems with H/kT = 7, ε_{sp}/kT = 2, δ = 3 Å, σ_{ion} = 6.94 Å, pH = 4, σ_p = 34.3 Å, and Δr = 0.08 Å for various values of ω_{PA}. The partition coefficient, K, increases exponentially with the ionic strength. This dependence is commonly observed feature in salting-out not only for proteins but also for other organic substances and dissolved gases. The exponential form has been used extensively in correlating protein salting-out data. Partition coefficient increases with the degree of pre-aggregation. It agrees with the previous theoretical results that large particles separate more efficiently.

Figure 3 shows the dependence of partitioning on square-well parameters δ and ε/kT. Both square-well depth and width give large effects on the protein partitioning. It means that specific interactions between protein molecules (e.g. hydrogen bonding, protein surface structure, etc.) play an important roll in the aggregation of protein molecules.

Coen *et al.* [6] have conducted precipitation experiments for two small globular proteins, hen-egg-white lysozyme and α-chymotrypsin in solutions of ammonium sulfate at various ionic strengths and pH. Figure 4 shows experimental and calculated values of $C_{p,super}$ and K as a function of ionic strength for the hen-egg-white lysozyme (at pH 4). Figure 4 represents the α-chymotrypsin data (at pH 8.3) for $C_{p,super}$ and K as a function of ionic strength. In those calculations, Hamaker constant and the value of, Δr, the thickness of the hydration/stern layer were 8.9 kT and 0.8 nm, respectively. These values are coincident with values reported by Kuhner,[27] who indicated that Hamaker constant depends on the value

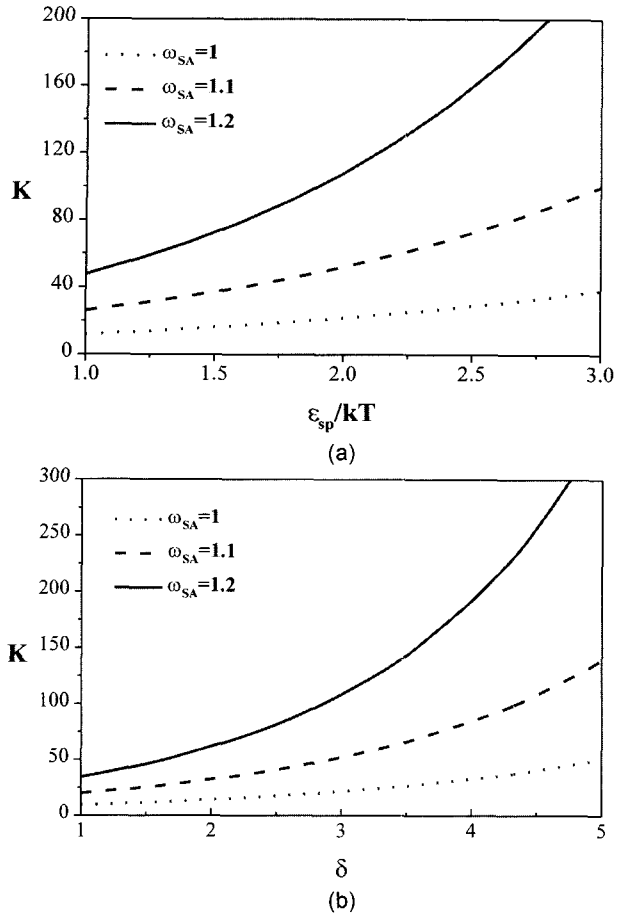

Figure 3. Effect of model parameter [ε_{sp}/kT (a), δ (b)]: H/kT = 8.9, ε_{sp}/kT = 2, δ = 0.3 nm, d_s = 0.694 nm, pH = 7, C_{salt} = 5 M, d = 3.34 nm.

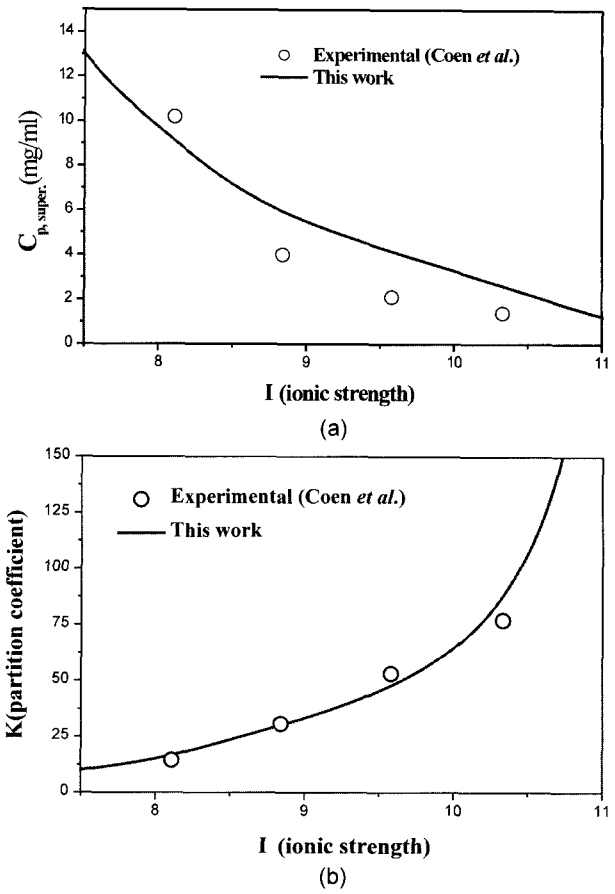

Figure 4. Experimental and correlated values of $C_{p,super}$ (a) and K (b) in the case of α-chymotrypsin in ammonium sulfate at pH 8.3: H/kT = 8.9, Δr = 0.08 nm, ε_{sp}/kT = 3.3, δ = 0.3 nm, d_s = 0.694 nm, d = 4.34 nm, ω_{PA} = 1.25. Dark squares are experimental data from Coen *et al.*[6] and the solid lines are calculated values using the proposed model.

of the thickness of the hydration/stern layer. As shown in Figure 5, calculated equilibrium coefficient and supernatant concentration are in qualitative agreement with experimental results of hen-egg-white lysozyme for ω_{PA} = 1.4, ε_{sp}/kT = 3.7 and δ = 4 Å. If the value of ω_{PA} = 1.4 is considered, 40% of lysozyme is pre-aggregated before the partitioning is processed. The proposed model also agrees very well with α-chymotrypsin experimental data for ω_{PA} = 1.25, ε_{sp}/kT = 3.3 and δ=3 Å. Considering ω_{PA} =1.25, it implies that 25% of the α-chymotrypsin is pre-aggregated before the partitioning process. Comparing ω_{PA} values for two model proteins presented in this study indicates that the effect of the specific interaction is more effective in lysozyme solution than that of α-chymotrypsin solution.

Binary Protein System. For aqueous mixtures of globular protein, we present reduced osmotic pressure-composition diagrams with various ionic strengths and given protein diameters.

Figure 6 shows the effect of the salt concentration for the systems with H/kT = 8.9, Δr = 0.08 nm ε_{sp}/kT = 0.2, δ = 0.3 nm, d_s = 0.694 nm, d_{11} = 3.5 nm and d_{22} = 3.4 nm. The solubility of globular proteins increases with the salt concentration. The composition difference between fluid and solid phases at the lower salt concentration is larger than that of the higher salt concenration. However, the results show that the salt concentration effect is small.

Figure 7 shows the effect of the size difference between protein-1 and protein-2 for the given system with H/kT = 8.9, Δr = 0.08 nm ε_{sp}/kT = 0.2, δ = 0.3 nm, d_s = 0.694 nm, and C_{salt} = 3 M for various d_{22} and fixed d_{11} = 3.5 nm. In the case of d_{11} = 3.5 nm and d_{22} = 3.4 nm, there is slight composition difference between the fluid and solid phase. The larger disparity in size between dissimilar proteins shows the lager composition difference between fluid and solid phases at the given composition in the fluid phase. The protein solubility decreases with increasing the size of protein-2. At fixed size of protein-1, the size of protein-2 increases with the mean size of protein. It is correspondent with the size effect of the

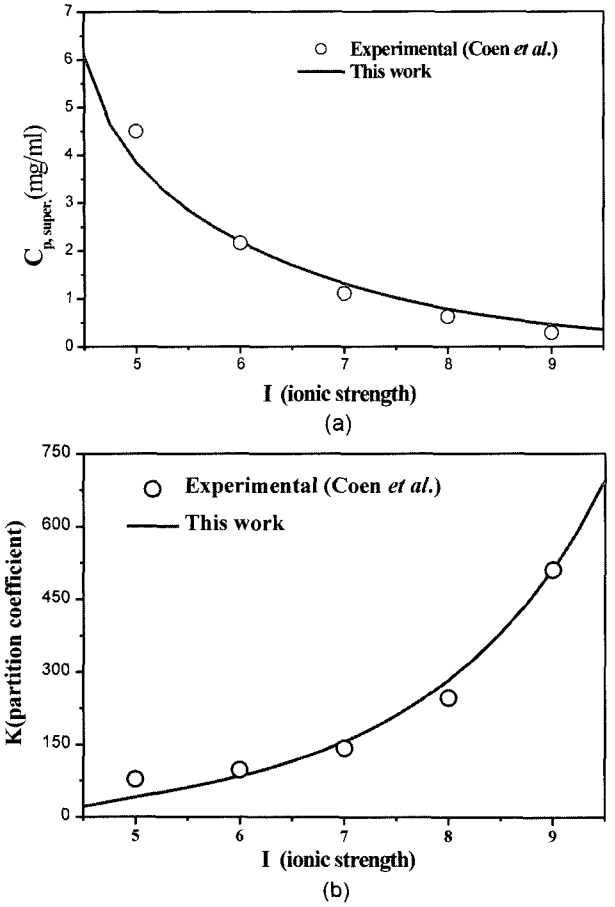

Figure 5. Experimental and correlated values of $C_{p,super}$ (a) and K (b) in the case of hen-egg-white lysozyme in ammonium sulfate at pH 4: $H/kT = 8.9$, $\Delta r = 0.08$ nm, $\varepsilon_{sp}/kT = 3.7$, $\delta = 0.4$ nm, $d_s = 0.694$ nm, $d = 3.43$ nm, $\omega_{PA} = 1.4$. Dark squares are experimental data from Coen *et al.*[6] and the solid lines are calculated values using the proposed model.

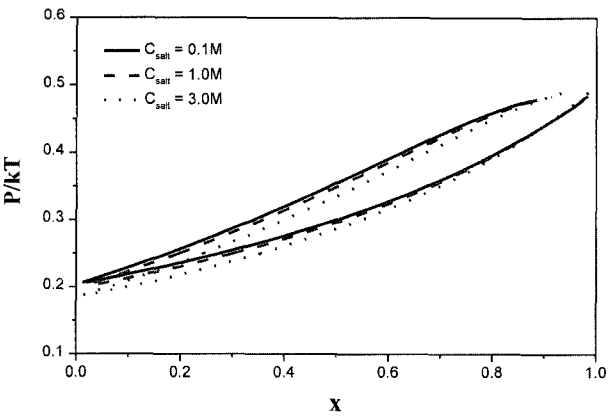

Figure 6. Theoretical phase diagrams for aqueous protein mixtures with different C_{salt} : $H/kT = 8.9$, $\Delta r = 0.08$ nm, $\varepsilon_{sp}/kT = 0.2$ nm, $\delta = 0.3$ nm, $d_s = 0.694$ nm, $d_{11} = 3.5$ nm, $d_{22} = 3.4$ nm.

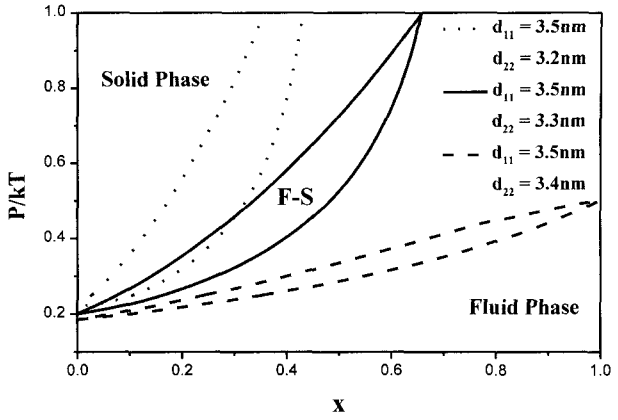

Figure 7. Theoretical phase diagrams for aqueous protein mixtures with different size d_{22} : $H/kT = 8.9$, $\Delta r = 0.08$ nm, $\varepsilon_{sp}/kT = 0.2$, $\delta = 0.3$nm, $d_s = 0.694$ nm, $C_{salt} = 3$ M.

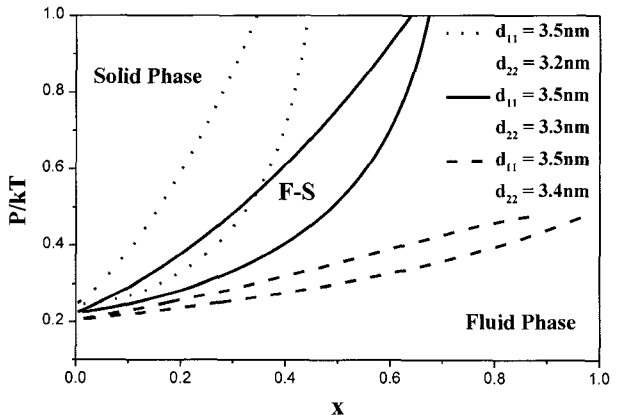

Figure 8. Theoretical phase diagrams for aqueous protein mixtures with different size d_{22} : $H/kT = 8.9$, $\Delta r = 0.08$ nm, $\varepsilon_{sp}/kT = 0.2$, $\delta = 0.3$ nm, $d_s = 0.694$ nm, $C_{salt} = 0.01$ M.

single protein system, that is, large solute molecules partition more strongly than those of small molecules.[28]

Figure 8 shows theoretical phase diagrams for the system with $H/kT = 8.9$, $\Delta r = 0.08$ nm $\varepsilon_{sp}/kT = 0.2$, $\delta = 0.3$ nm, and $d_s = 0.694$ nm for various d_{22} and fixed $d_{11} = 3.5$ nm at the salt concentration $C_{salt} = 0.1$ M. Comparing with each system of Figure 7 in the same size disparity, the difference of equilibrium composition between solid and fluid phase is greater than that of Figure 7. It agrees with the previous result shown in Figure 6.

Conclusions

We proposed a thermodynamic model to describe the salt-induced protein precipitation based on effective potentials of mean force. The model is developed based on a statistical mechanical perturbation theory and the reference term is

derived from the modified *Chiew*'s equation for the fluid phase and Young's equation for the solid phase. In a single protein system, model predictions indicate that the electrolyte concentration plays a primary role in affecting phase separation. The protein partition coefficient, K, increases exponentially with the ionic strength. Our results show that the pre-aggregation effect of protein plays an important role in the precipitation of proteins. Calculated equilibrium supernatant concentration and partition coefficient are in qualitative agreement with experimental results for both hen-egg-white lysozyme and α-chymotrypsin in solutions of ammonium sulfate when the effect of the pre-aggregation is considered.

In the binary protein system, we consider two effects on the phase separation. The composition difference between fluid and solid phases at a given composition of the fluid phases decreases with increasing the value of the disparity in protein size and the salt concentration. Further, the protein size difference is more effective than that of the salt concentration on the phase behaviors of protein/salt systems.

Appendix

Contributions to the effective two-body potentials for proteins in aqueous electrolyte solution.

1. The electric double-layer repulsion[7,27]:

$$\frac{W_{ij}^{elec}(r)}{kT} = \frac{z_i z_j e^2}{4\pi\varepsilon_o\varepsilon_r kT}\frac{e^{[-\kappa(r-d_p)]}}{r\left(1+\frac{\kappa d_{ii}}{2}\right)\left(1+\frac{\kappa d_{jj}}{2}\right)} \quad \text{for } r > (d_{ij}+2\Delta r) \tag{A1}$$

k : Boltzmann constant
T : absolute temperature
z_i : valence of the species i
e : the unit of electron charge
d_{ii} : the diameter of species i
$d_{ij} = (d_{ii}+d_{jj})/2$
$4\pi\varepsilon_0$: the dielectric permittivity of free space
ε_r: the relative dielectric permittivity of water
Δr : the effective-sphere hydration/stern layer
κ: the inverse of the Debye length; given by $\kappa^2 = (2e^2N_AI)/(kT\varepsilon_0\varepsilon)$
N_A : Avogadros number
I : the ionic strength of the salt, given by $I = (z^2_{an}\rho_{an}+z^2_{cat}\rho_{cat})/2$
z_{an} and z_{cat} : the anion and cation valences, respectively
ρ_{an} and ρ_{cat} : the ionic number densities.

2. The attractive Hamaker dispersion interaction[7,29]:

$$\frac{W_{ij}^{disp}(r)}{kT} = -\frac{H}{6}\left[\frac{d_{ii}d_{jj}}{r^2-d_{ij}^2}+\frac{d_{ii}d_{jj}}{r^2-\frac{(d_{ii}-d_{jj})^2}{4}}+2ln\left[\frac{r^2-d_{ij}^2}{r^2-\frac{(d_{ii}-d_{jj})^2}{4}}\right]\right] \quad \text{for } r > d_p+2\Delta r \tag{A2}$$

H : the effective Hamaker constant for the protein-protein interaction

3. The osmotic attractive interaction potential[16,27]:

$$\frac{W_{ij}^{osmotic}(r)}{kT} = -\frac{2\pi\rho_s}{3}\left[\left(\frac{d_{iis}}{2}\right)^3+\left(\frac{d_{jjs}}{2}\right)^3\right] \times\left[1+\frac{r^3}{8\left[\left(\frac{d_{iis}}{2}\right)^3+\left(\frac{d_{jjs}}{2}\right)^3\right]}-\frac{3r}{4}\frac{\left[\left(\frac{d_{iis}}{2}\right)^2+\left(\frac{d_{jjs}}{2}\right)^2\right]}{\left[\left(\frac{d_{iis}}{2}\right)^3+\left(\frac{d_{jjs}}{2}\right)^3\right]}-\frac{3}{8r}\frac{\left[\left(\frac{d_{iis}}{2}\right)^2+\left(\frac{d_{jjs}}{2}\right)^2\right]^2}{\left[\left(\frac{d_{iis}}{2}\right)^3+\left(\frac{d_{jjs}}{2}\right)^3\right]}\right]$$

$$\text{for } d_{ij} < r < d_{ijs}+2\Delta r \tag{A3}$$

ρ_s : the total ionic number density
$d_{iis} = (d_{ii} + d_s)/2$
$d_s = (z_{an}d_{cat} + z_{cat}d_{an})/(z_{cat}+z_{an})$: a valence-weighted ion diameter

4. The specific interaction[20,27]:

$$\frac{W_{specific}(s)}{kT} = -\frac{\varepsilon_{sp}}{kT} \quad for \quad d_p < r < (d_p+\delta) \tag{A4}$$

ε_{sp} and δ : model parameters

References

(1) P. R. Foster, P. Dunhill, and M. D. Lilly, *Biochem. Biophys. Acta*, **317**, 505 (1975).
(2) R. N. Haire, W. A. Tisel, J. C. White, and A. Rosenberg, *Biopolymers*, **23**, 2761 (1984).
(3) Y. C. Shih, H. W. Blanch, and J. M. Prausnitz, *Biotech. Bioeng.*, **40**, 1155 (1992).
(4) M. Q. Niederauer and C. E. Glatz, *Adv. Biochem. Eng. Technol.*, **47**, 159 (1992).
(5) F. Rothstein, in *Protein Precipitation Process Engineering*, R. G. Harrion, Ed., Dekker, New York, 1994.
(6) C. J. Coen, H. W. Blanch, and J. M. Prausnitz, *AIChE J.*, **41**, 1 (1995).
(7) E. Verwey and J. Overbeek, *Theory of Stability of Lyophobic Colloids*, Elsevier, Amsterdam, 1948.
(8) S. Askura and F. Oosawa, *J. Polym. Sci.*, **33**, 183 (1958).
(9) A. Vrij, *Pure & Appl. Chem.*, **48**, 471 (1976).
(10) J. F. Joanny, L. Leibler, and P. G. de Gennes, *J. Polym. Sci., Polym. Phys. Ed.*, **17**, 1073 (1979).
(11) H. De Hek and A. Vrij, *J. Colloid Interf. Sci.*, **41**, 996 (1995).
(12) A. P. Gast, C. K. Hall, and W. G. Russel, *J. Farad. Discuss. Chem. Soc.*, **76**, 189 (1983b).
(13) M. J. Grimson, *J. Chem. Soc. Farad. Trans.*, **79(2)**, 817 (1983).

(14) J. M. Victor and J. P. Hansen, *J. Phys. Lett.*, **45**, L-307 (1984).
(15) H. Mahadevan and C. K. Hall, *AIChE J.*, **36**, 1517 (1990).
(16) H. Mahadevan and C. K. Hall, *AIChE J.*, **38**, 573 (1992).
(17) V. Vlachy and J. M. Prausnitz, *J. Phys. Chem.*, **96**, 6465 (1992).
(18) V. Vlachy and H. W. Blanch, and J. M. Prausnitz, *AIChE J.*, **39**, 215 (1993).
(19) Y. C. Chiew, *Molec. Phys.*, **70**, 129 (1990).
(20) D. Kuehner, H. W. Blanch, and J. M. Prausnitz, *Fluid Phase Equilibria,* **116**, 140 (1996).
(21) S. Asakura and F. Oosawa, *J. Chem. Phys.*, **22**, 1255 (1954).
(22) A. P. Gast, C. K. Hall, and W. G. Russel, *J. Colloid Interf. Sci.*, **96**, 251 (1983a).
(23) J. M. Prausnitz, R. N. Lichtenthaler, and E. G. D. Azevedo, *Molecular Thermodynamics of Fluid Phase Equilibria*, Prentice-Hall, Englewood Cliffs, NJ., 1986.
(24) D. A.Young, *J. Chem. Phys.*, **98**, 9819 (1993).
(25) Y. Song, S. M. Lambert, and J. M. Prausnitz, *Ind. Eng. Chem. Res.*, **33** (1994).
(26) N. F. Carnahan and K. E. Starling, *J. Chem. Phys.*, **51**, 635 (1969).
(27) D. Kuehner, C. Heyer, C. Ramsch, U. M. Fornefeld, H. W. Blanch, and J. M. Prausnitz, *Biophysical J.*, **73**, 3211 (1997).
(28) P. A. Albertsson, *Partition of Cell Particles and Macromolecules*, Wiley, New York, 1986.
(29) H. C. Hamaker, *Physica IV,* **10**, 1058 (1937).
(30) S. G. Kim and Y. C. Bae, *Korean J. Chem. Eng.*, **17(6)**, 638 (2000).
(31) R. A. Curtis, C. Steinbrecher, M. Heinemann, H. W. Blanch, and J. M. Prausnitz, *Biophysical Chemistry*, **98**, 249 (2002).